OPTIMAL DESIGN OF MFL SENSOR FOR DETECTING BROKEN STEEL STRANDS IN OVERHEAD POWER LINE

X. L. Jiang, Y. F. Xia*, J. L. Hu, F. H. Yin, C. X. Sun, and Z. Xiang

State Key Laboratory of Power Transmission Equipment & System Security and New Technology, College of Electrical Engineering, Chongqing University, Chongqing 400030, China

Abstract—Aluminum conductor steel-reinforced (ACSR) cable is a specific type of stranded cable typically used for electrical power delivery. Steel strands in ACSR cable play a supportive role for overhead power line. Inspection timely is an important means to insure safety operation of power lines. As steel strands are wrapped in the center of ACSR cable, the common artificial inspection methods with optical instruments are limited to find inner flaws of power line. Recently, inspection of power line by robot with detectors is a method with good prospect. In this paper, the optimal design model of detector based on magnetic leakage flux (MLF) carried by robot for detecting broken steel strands in ACSR cables has been proposed. The optimal design model of MFL sensor is solved by niche genetic algorithm (NGA). Field experiment results show that the design method of the detector can be applied to different types of ACSR cables. The magnitude field induced by transmission current has nearly no influences on the detection of broken steel strands, and the developed detector carried by robot can identify broken steel strands with high reliability and sensitivity.

1. INTRODUCTION

ACSR is mainly composed of some twisted aluminum lines in the outer layer and some steel strands in the center. The outer strands of ACSR cable are aluminum, chosen for its excellent conductivity, low weight and low cost. The center strand of ACSR cable is of steel

for the strength required to support the weight without stretching the aluminum due to its ductility. This gives the cable an overall high tensile strength. So broken steel strands in ACSR cables have a very strong impact on the safe operation of power grids. During the long-term outer door field service, ACSR cables may be damaged by lightning strike, corrosion of chemical contaminants, ice-shedding, wind vibration of conductors, lines' galloping and external forces' destroy and so forth [1–5]. It will induce some fatal accidents if the latent faults cannot be recognized and restored as early as possible. To ensure the safe operation, power lines should be inspected routinely. The common means to be used for latent faults inspection in power lines is manual examination with hand-held devices such as telescope by workers. This method is not only labor-intensive but also in low precision. Aerial maintenance of power line by helicopter is efficient but also dangerous [6, 7]. Recently, with the development of both artificial intelligence technologies and smart grid, inspection of power line by robot with detectors is a method with good prospect [8–10].

Genetic algorithm (GA) is a kind of optimization algorithm simulates biological heredity and evolutionary processes. GA has advantages in solving constrained nonlinear optimization problem with parallelism, global search and self-adaptation [11]. So GA is becoming a valuable tool for the analysis of signals in many applications [12–21]. Traditional simple genetic algorithm (SGA) trends to trap in local optimization as a result of the elitist strategy and the selection strategy based on proportion. Niche genetic algorithm (NGA) is a kind of modified GA improved by adaptive technology [22, 23] and niche selection technology [24, 25].

In this study, the optimal design model of detector based on magnetic leakage flux (MLF) carried by robot for detecting broken steel strands in ACSR cables has been proposed. The optimal design model of MFL sensor is solved by niche genetic algorithm (NGA). The possibility to detect the defects in power line is then studied by field experiment. And the influence of magnetic field induced by transmission current in ACSR cable to the detector is analyzed.
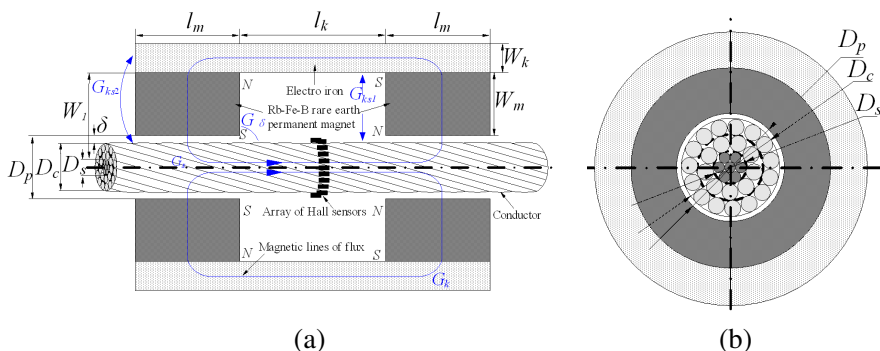
2. STRUCTURE OF MFL SENSOR

2.1. Principle of Detecting Broken Steel Strands by MLF Sensor

The principle of detecting broken steel strands is shown in Figure 1. As the steel twisted line in ACSR cable is made of ferromagnetism material, the steel strands can be magnetized adequately by rare earth permanent magnet. Magnetic circuit can be formed by permanent
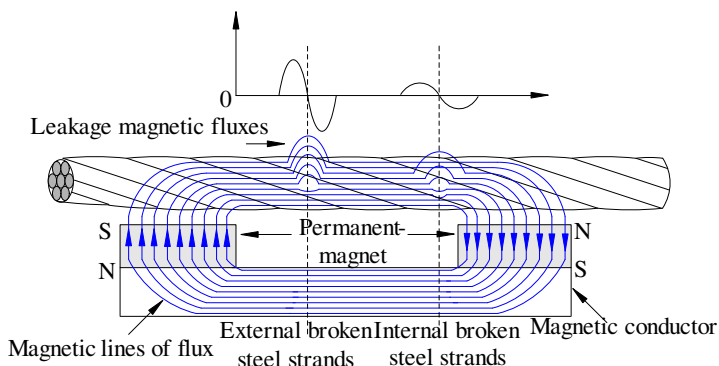
Figure 1. Principle of detecting broken steel strands in ACSR by MLF sensor.

Figure 2. Structure of MLF sensor carried by inspection robot.

magnet, magnetic conductor and steel strands. When there are broken steel strands in ACSR cable, the decrease of magnetic permeability at the position of broken steel strands results in leakage of the magnetic field fluxes to the surrounding atmosphere. The MFL can be detected by the magneto-electric transducer such as Hall sensor.

2.2. The Structure of MFL Sensors

The sensor based on MFL principle for detecting broken steel strands in ACSR cable is composed of magnetic source, magnetic conductor, data acquisition card, array of Hall elements and corresponding signal conditioning circuits. In the proposed detection scheme, the steel strands in ACSR cable can be magnetized by rare earth permanent magnet of $48^{\#}$ Rb-Fe-B, the electrical pure iron is utilized as magnetic

conductor. The structure of MFL sensors is shown in Figure 2. Where, D_s, D_c and D_p are the external diameter of steel strands in ACSR cable, the external diameter of ACSR cable and inner diameter of permanent-magnet, respectively (in mm). S_s is the sectional area of steel strands in power line (in mm^2). D_{ms} is the diameter of steel rod with the sectional area S_s, and $D_{ms} = \sqrt{4S_s/\pi}$. δ is the distance between the inner surface of rare earth permanent magnet and the outer surface of electrical conductor (in mm). δ' is distance between the inner surface of permanent-magnet and external surface of steel strands in ACSR cable (in mm), and $\delta' = (D_p - D_{ms})/2$. l_m is the length of permanent-magnet along power line (in mm). l_k is the distance between the inside of two permanent-magnets (in mm). W_m and W_k are the radial thickness of permanent-magnet and the radial thickness of magnetic conductor, respectively (in mm). W_1 is the distance from the outer surface of steel strands in ACSR cable to the inner surface of magnetic conductor (in mm), and $W_1 = W_m + \delta'$.

2.3. Equivalent Magnetic Circuit for MFL Sensor

The structure of equivalent magnetic circuit is shown in Figure 3. Where, G_δ is the magnetic conductance of the air gap between the inner surface of permanent-magnet and external surface of the steel strands in ACSR cable. G_{ks} is the magnetic conductance of the air gap between the inner surface of magnetic conductor and the external surface of the steel strands in ACSR cable. G_s is the magnetic conductance of steel strands. G_k is the magnetic conductance of electro iron. The magnetic

(a) The equivalent magnetic circuit   (b) Simplified magnetic circuit
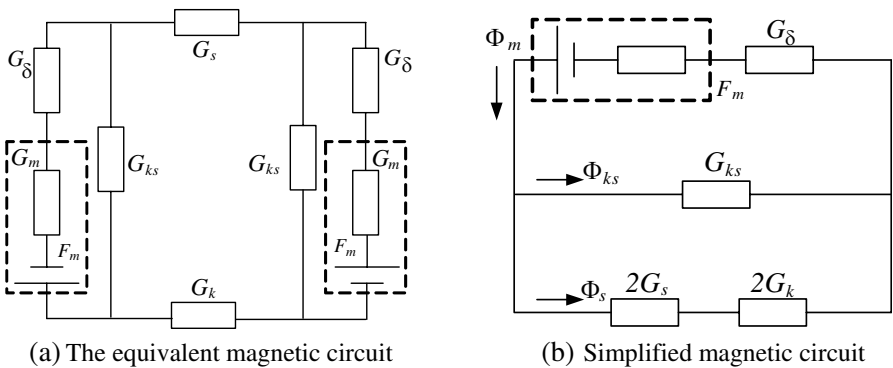
Figure 3. Equivalent magnetic circuit of MFL sensor.

conductance can be expressed as follows [26]:

$$
\begin{cases}
G_\delta = \dfrac{2\pi\mu_0 l_m}{\ln\left(1 + \delta/r\right)} = \dfrac{2\pi\mu_0 l_m}{\ln(D_p/D_{ms})} \\[2mm]
G_{ks} = 4\mu_0 \left[D_{ms} + \sqrt{W_l\left(W_l + W_k\right)}\ln\left(1 + \frac{W_k}{W_l}\right)\right] \\[2mm]
G_s = \mu_{rs}\left(B_s\right)\pi D_{ms}^2 \big/ (4l_k) \\[2mm]
G_k = \mu_{rk}\left(B_k\right)\pi W_k \left(D_{ms} + 2W_l + W_k\right)/(l_k)
\end{cases}
\tag{1}
$$

Based on the Kirchhoff's theory and Figure 3, the magnetic conductance and flux satisfies:

$$
\begin{cases}
\dfrac{1}{G_{ks}}\phi_{ks} = H_m W_m - \dfrac{1}{G_\delta}\phi_m \\[3mm]
\dfrac{1}{G_{ks}}\phi_{ks} - \dfrac{1}{2}\left(\dfrac{1}{G_s} + \dfrac{1}{G_k}\right)\phi_s = 0
\end{cases}
\tag{2}
$$

where, ϕ_m is the flux of permanent-magnet (in Wb), ϕ_s is the flux of steel strands in ACSR cable (in Wb), and the flux can be expressed as:

$$
\begin{cases}
\phi_m = \int_S \mathbf{B}_m \cdot d\mathbf{S} = B_m S_m \\[2mm]
\phi_s = \int_S \mathbf{B}_s \cdot d\mathbf{S} = \int_k \mathbf{B}_k \cdot d\mathbf{S} = B_s S_s \\[2mm]
\phi_m = \phi_{ks} + \phi_s
\end{cases}
\tag{3}
$$

Then the magnetic induction density of steel strands in ACSR cable can be calculated as:

$$
B_s = \frac{1}{S_s}\left[B_m S_m \left(1 + \frac{G_{ks}}{G_\delta}\right) - H_m W_m G_{ks}\right]
\tag{4}
$$

where, H_m and B_m are coercive force and residual magnetism of N48$^\#$ Nd-Fe-B rare-earth permanent magnet at the operation point, respectively. The relative permeability of N48$^\#$ Nd-Fe-B rare-earth permanent magnet is $\mu_r = 1.0524$. The demagnetization curve of Nd-Fe-B rare-earth permanent magnet is a straight line. In order to ensure the operation point of permanent magnet exists above the break point of demagnetization curve and leaves a certain degree, the operating point of Nd-Fe-B is assigned to $0.85B_r$, at this time $B_m = 0.6\,\mathrm{T}$, $H_m = 644.85\,\mathrm{KA/m}$.

The magnetic field vector of the position at which magneto-electric transducer is placed can be calculated as:

$$
\mathbf{B} = \frac{\pi B_s d_g^2}{16\pi \mathbf{r}^2}
\tag{5}
$$

where, $\mathbf{r}$ is the distance vector from the position of broken steel strands to the position at which magneto-electric transducer is placed (in mm). d_g is the diameter of equivalent magnetic charge for broken

steel strands. The broken steel strands can be equivalent to a couple of magnetic charges [27].

It can be seen from Figure 2 and formula (5) that a magnetic circuit is composed of permanent magnet, magnetic conductor and steel strands. The sectional area S_s of the position where there are broken strands decreases. And the magnetic induction intensity B_s of the position where there are broken strands increases correspondingly. So the magnetic field vector **B** of the position at which magneto-electric transducer is placed increases. And then quantitative diagnose of broken steel strands can be realized by the MFL data acquired.

3. OPTIMIZATION DESIGN MODEL

3.1. Relationship Between the Weight and Structural Parameter of MFL Sensor

The volumes of permanent magnet and magnetic conductor can be calculated respectively as follows:

$$V_m = 2\pi l_m \left(D_p W_m + W_m^2 \right) \tag{6}$$

$$V_k = \pi \left(2l_m + l_k \right) \left[W_k^2 + \left(D_p + 2W_m \right) W_k \right] \tag{7}$$

And then the weight of MFL sensor can be calculated as:

$$M = \rho_m V_m + \rho_k V_k \tag{8}$$

where, ρ_m is the density of $48^{\#}$ Rb-Fe-B permanent magnet, and $\rho_m \approx 7.5\,\text{g/cm}^3$; ρ_k is the density of electrical pure iron, and $\rho_k \approx 7.87\,\text{g/cm}^3$.

3.2. Constraints Condition

According to the analysis above, only if steel strands in ACSR cable are magnetized adequately, the leakage of the magnetic field fluxes to the surrounding atmosphere can be detected by the magneto-electric transducer such as Hall sensor. The literature [28] proposed that the inner flaws in cylindrical steel material can be detected by the MFL method if the magnetic induction intensity in cylindrical steel material is bigger than 1.4 T and the magnetic ability of magnetic conductor is bigger than that of steel strands in ACSR cable. So the magnetic induction intensity in steel strands B_s, the magnetic conductance of steel strands G_s and the magnetic conductance of magnetic conductor G_k satisfy:

$$B_s = g_1 \left(W_m, W_k, l_m, l_k \right) \geq 1.4 \tag{9}$$

$$G_k - G_s = g_2 \left(W_m, W_k, l_m, l_k \right) \geq 0 \tag{10}$$

Considering the portability of MFL sensor for power line inspection robot, the distance from the inner surface of permanent magnet to the external surface of magnetic conductor satisfies:

$$W_m + W_k = g_3 (W_m, W_k, l_m, l_k) \leq 0.1 \tag{11}$$

In order to reduce the influence of MFL between the inner surface of permanent magnet and external surface of steel strands to the detection of broken strands, the length of steel strands magnetized evenly along the power line is bigger than the distance between the centers of two steel strands. So the length of steel strands magnetized evenly along the power line l_k satisfies [26, 27]:

$$l_{mm} + 2l_{ms} \leq l_k \leq 0.2 \tag{12}$$

where, l_k is the length of steel strands magnetized evenly along the power line (in mm), l_{mm} is the distance between the centers of two steel strands (in mm). l_{ms} is the shortest distance between inside of permanent magnet and the external surface of steel strands whose magnetic induction density of normal component is nearly zero (in mm). In this study, l_{mm} approximately equals 4.8 mm, l_{ms} is no more than 35 mm.

In order to ensure sufficient magnetization of steel strands, the length of permanent-magnet along power line l_m satisfies [26]:

$$D_s + 0.005 \leq l_m \leq l_k \tag{13}$$

4. STRUCTURAL PARAMETERS OF MFL SENSOR OPTIMIZED BY NGA

4.1. Fitness Function for GA

It is can be seen from the structure of MFL sensor and the corresponding equivalent magnetic circuit that optimized design of MFL sensor is a constrained nonlinear optimization problem. When the structure parameters of MFL sensor solved by GA can not meet the performance requirements, a penalty factor p is constructed to punish the objective function. Since the sensor's lightest weight serves as the objective function, it is necessary to adjust the fitness function as [11]:

$$f = p \left[M_{\max} - CM (x) \right] \tag{14}$$

where, $M_{\max}$ is an estimated maximum weight (in kilogram), and it is set as 20 kg in this program. C is the duplicated number of expectative optimal individuals, and it is usually set as $1.2 \sim 2$ [11]. $M(x)$ is the calculated weight of MFL sensor (in kilogram). Penalty factors p can be set as:

$$p = \begin{cases} 1 & B_s \geq 1.4 \text{ and } G_k \geq G_s \\ 0 & B_s \leq 1.4 \text{ or } G_k \leq G_s \end{cases} \tag{15}$$
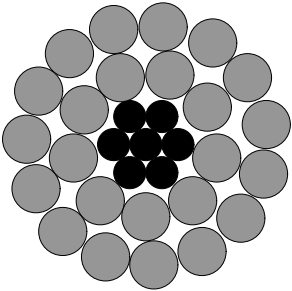
4.2. Objective Function

Power line is inspected by robot with different kinds of detectors. As lower cost and more detectors with less weight can be carried by power line inspection robot, the MFL sensor's weight serves as the objective function. In this study, the optimized structural parameters of MFL sensor with the objective function of the lightest weight is compared with the optimized structural parameters of MFL sensor with the objective function of the largest magnetic induction density in steel strands.
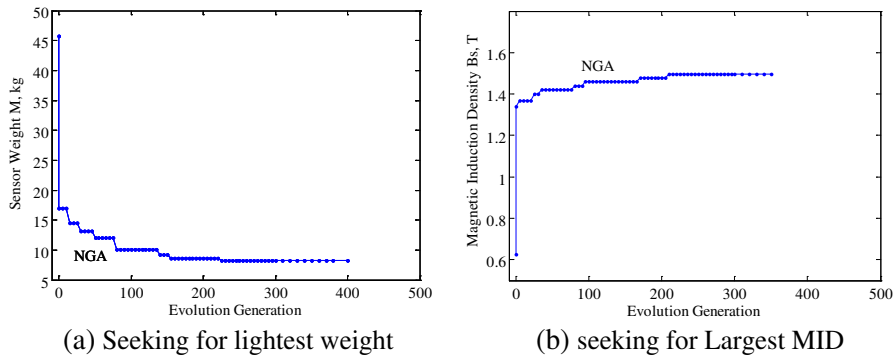
4.3. Result of Optimization

In this study, a prototype of MFL sensor has been developed for detecting broken steel strands in ACSR cable of LGJ-240. The ACSR cable of LGJ-240 has been widely used as overhead power line of 220 kV to 500 kV in China. LGJ-240 is composed of 24 twisted aluminum wires in the outer layer and 7 twisted steel wires in the center. The profile and parameters of LGJ-240 are shown in Table 1. The structural parameters of MFL sensor has been designed and optimized by NGA.

The sensor's lightest weight serves as the objective function, and the specific optimization process of applying NGA for optimized design of MFL sensor is shown in Figure 4(a). The largest magnetic induction density in steel strands serves as the objective function (the weight of MFL sensor is no more than 20 kg), and the specific optimization process of applying NGA for optimized design of MFL sensor is shown in Figure 4(b). It can be seen from Figure 4 that the objective function value varies obviously in the preliminary stage, and then it trends to

Table 1. Parameters of specimen.

| Type of Sample	LGJ-240
Diameter : D_c=21.6 mm	
Diameter of steel strands: D_s=7.2 mm	
Diameter of single twisted steel wire: d_s=2.4mm	
Diameter of single twisted aluminum wire: d_a=3.6mm	
Number of steel strands:7	
Number of aluminum strands:24	

(a) Seeking for lightest weight

(b) seeking for Largest MID

Figure 4. Evolutionary process of NGA.

Table 2. Result of optimization.

Item	Structure Parameters /mm				B_s/T	M/kg
	W_m	l_m	W_k	l_k		
Original	30.00	31.25	20.00	80.00	1.51	10.56
Weight as Objective Function	30.19	25.10	16.50	75.00	1.41	7.66
MID as Objective Function	35.50	30.15	18.10	75.00	1.56	11.61

be a steady value after generations (Evolution generation > 300 in Figure 4(a), and Evolution generation > 200 in Figure 4(b)).

The optimized structural parameters of MFL sensor with the objective function of the lightest weight is compared with the optimized structural parameters of MFL sensor with the objective function of the largest magnetic induction density (MID) in steel strands. The comparison of the original parameters, optimized parameters by NGA are shown in Table 2. The original designed parameters are based on the references [26, 27]. It can be seen from the Table 2 that the MID in steel strands increases with the radial thickness of permanent-magnet W_m and the length of permanent-magnet along power line l_m, the MID in steel strands decreased with the radial thickness of magnetic conductor W_k and the distance between the inside of two permanent-magnets l_k. The weight of MFL sensor reduces 27.5% and MID in steel strands reduces only 6.6% compared with original parameters

(a) Prototype of MFL sensor probe   (b) Prototype of signal processing circuit
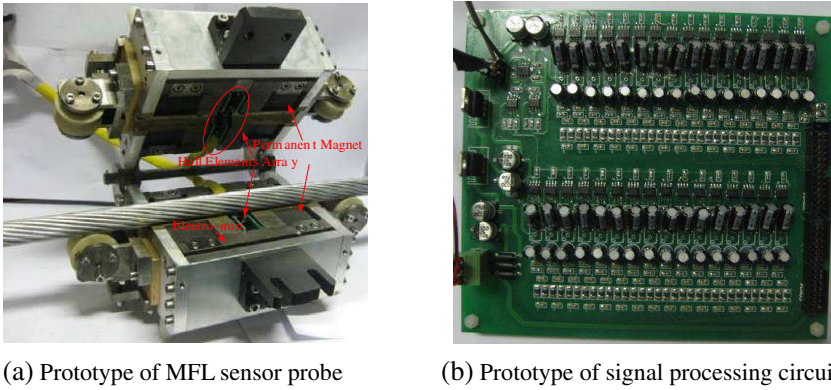
Figure 5. Prototype of MFL sensor.

Figure 6. Field test of inspection robot with MFL sensor.

when the lightest weight serves as the objective function. The MID in steel strands only increases 3% and the weight of MFL sensor increases 10% when the MID in steel strands serves as the objective function. It can also be seen that the further increase of MID in steel strands will make the weigh of MFL sensor increases obviously when the MID in steel strands is high yet. The increase of weight of MFL sensor will decrease the inspection robot's carrying ability and increase the cost of MFL sensor and robot. So the weight of MFL sensor should be as the objective function on condition that the steel strands in ACSR cable can be magnetized adequately.

Based on the optimized parameters of MFL sensor, a prototype has been produced and shown in Figure 5. The signal processing circuit in Figure 5(b) is composed of power amplifier, filter circuits adding circuits, etc. Then the original detection signals of the Hall elements array in Figure 5(a) can be amplified and added, and the noises can be suppressed.
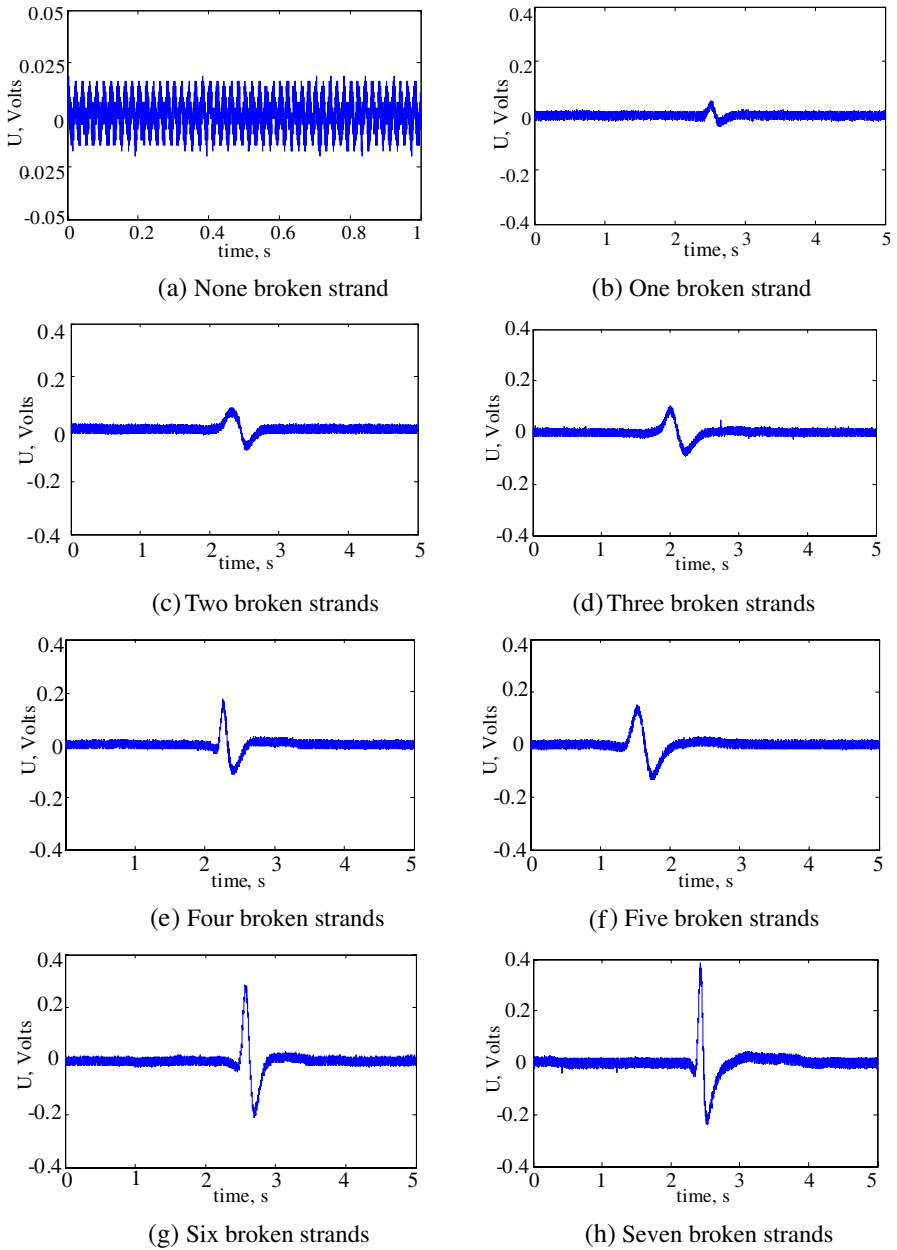
Figure 7. Detection signal of broken strands in ACSR.

5. FIELD EXPERIMENT

Field experiment is shown in Figure 6, and the experiment was processed in Xuefeng Mountains, Huaihua, Hunan, China. The field experiment base was built by Chongqing University under the key project of Chinese national programs for fundamental research and development (973 Program). The specimen of LGJ-240 is inspected by robot with MFL sensor and other detectors. In this study, the single power line is applied with AC current of 500 A at 50 Hz.

The detection signal of MFL sensor for detecting broken strands in ACSR cable of LGJ-240 is analyzed in this study to show the validity and feasibility of the detection scheme. The detection signals of MFL sensor obtained in experiments are shown in Figure 7. It is can be seen from Figure 7, (1) the detection accuracy is sufficient to locate flaws of one half the size of one strand; (2) the detection signal of magnitude field induced by transmission current is smaller than the signal of one broken strand, so the magnitude field induced by transmission current has very small influence on the detection of broken steel strands in power line; (3) the amplitude of detection signal varies with the number of broken strands, the more broken steel strands in power line, the more the variation of detection signal.

6. CONCLUSION

(1) The structural style and optimal design method of the MFL sensor can be applied to teh design of MFL sensor for other types of ACSR cable. The specific parameters of MFL sensor probe can be determined by the type of power line.

(2) The optimal design model of detector based on magnetic leakage flux (MLF) carried by robot for detecting broken steel strands in ACSR cables has been proposed. The optimal design model of MFL sensor can be solved by NGA.

(3) The increase of weight of MFL sensor will decrease the inspection robot's carrying ability and increase the cost of MFL sensor and robot. So the weight of MFL sensor should be as the objective function on condition that the steel strands in ACSR cable can be magnetized adequately.

(4) The exterior disturbance has no impact on the performance of MFL sensor for detecting broken strands in power line, and the magnitude field induced by transmission current has nearly no influence on the detection of broken strands in power line. So the developed MFL sensor can detect broken steel strands with high stability.

(5) The detection accuracy is sufficient to locate flaws of one half the size of one strand, which is adequate for user requirements. So the developed MFL sensor can detect broken steel strands with high sensitivity.

ACKNOWLEDGMENT

REFERENCES

1. Lings, R., D. Cannon, L. Hill, M. Gaudry, R. Stone, and R. Shoureshi, *Inspection* & *Assessment of Overhead Line Conductors*, A State-of-the Science Report, EPRI Technical Progress 1000258, Electric Power Research Institute, Palo Alto, California, USA, 2000.

2. Goda, Y., S. Yokoyama, S. Watanabe, T. Kawano, and S. Kanda, "Melting and breaking characteristics of OPGW strands by lightning," *IEEE Transactions on Power Delivery*, Vol. 19, No. 4, 1734–1740, 2004.

3. Kudzys, W., "Safety of power transmission line structures under wind and ice storms," *Engineering Structures,* Vol. 28, 682–689, 2006.

4. Isozaki, M., K. Adachi, T. Hita, and Y. Asano, "Study of corrosion resistance improvement by metallic coating for overhead transmission line conductor," *Electrical Engineering in Japan*, Vol. 163, No. 1, 41–47, 2008.

5. Azevedo, C. R. F. and T. Cescon, "Failure analysis of aluminum cable steel reinforced (ACSR) conductor of the transmission line crossing the paraná river," *Engineering Failure Analysis*, Vol. 9, No. 4, 645–664, 2002.

6. Cameron, G. W., P. S. Bodger, and J. J. Woudberg, "Incomplete faraday cage effect of helicopters used in platform live-line maintenance," *IEE Proceedings-Generation, Transmission and Distribution*, Vol. 145, No. 2, 145–148, 1998.

7. Ashidater, S., S. Murashima, and N. Fujii, "Development of a helicopter-mounted eye-safe laser radar system for distance measurement between power transmission lines and nearby trees," *IEEE Transactions on Power Delivery*, Vol. 17, No. 2, 644–648, 2002.

8. Sawada, J., K. Kusumoto, Y. Maikawa, T. Munakata, and Y. Ishikawa, "Mobile robot for inspection of power transmission lines," *IEEE Transactions on Power Delivery*, Vol. 6, No. 1, 309–315, 1991.

9. Toussaint, K., N. Pouliot, and S. Montambault, "Transmission line maintenance robots capable of crossing obstacles: Stage-of-the-art review and challenges ahead," *Journal of Field Robotics*, Vol. 26, No. 5, 477–499, 2009.

10. Li, W. H., A. Tajbakhsh, C. Rathbone, and Y. Vashishtha, "Image processing to automate condition assessment of overhead line components," *2010 1st International Conference on Applied Robotics for the Power Industry*, 5–7, Delta Centre-Ville, Montréal, Canada, Oct. 1–6, 2010.

11. Chen, L., Y. Luo, H. Chen, and L. Zhang, *Genetic Algorithm for Mechanical Optimum Design*, 1st edition, China Machine Press, Beijing, China, 2005 (in Chinese).

12. Siakavara, K., "Novel fractal antenna arrays for satellite networks: Circular ring Sierpinski carpet arrays optimized by genetic algorithms," *Progress In Electromagnetics Research*, Vol. 103, 115–138, 2010.

13. Jian, L., G. Xu, J. Song, H. Xue, D. Zhao, and J. Liang, "Optimum design for improving modulating-effect of coaxial magnetic gear using response surface methodology and genetic algorithm," *Progress In Electromagnetics Research*, Vol. 116, 297–312, 2011.

14. Reza, A. W., M. S. Sarker, and K. Dimyati, "A novel integrated mathematical approach of ray-tracing and genetic algorithm for optimizing indoor wireless coverage," *Progress In Electromagnetics Research*, Vol. 110, 147–162, 2010.

15. Mahanti, G. K., N. Pathak, and P. K. Mahanti, "Synthesis of thinned linear antenna arrays with fixed sidelobe level using real-coded genetic algorithm," *Progress In Electromagnetics Research*, Vol. 75, 319–328, 2007.

16. Xu, O., "Collimation lens design using AI-GA technique for Gaussian radiators with arbitrary aperture field distribution," *Journal of Electromagnetic Waves and Applications*, Vol. 25, No. 5–6, 743–754, 2011.

17. Zhang, Y.-J., S.-X. Gong, X. Wang, and W.-T. Wang, "A hybrid genetic-algorithm space-mapping method for the optimization of broadband aperture-coupled asymmetrical u-shaped slot antennas," *Journal of Electromagnetic Waves and Applications*, Vol. 24, No. 16, 2139–2153, 2010.

18. Dadgarnia, A. and A. A. Heidari, "A fast systematic approach for microstrip antenna design and optimization using ANFIS and GA," *Journal of Electromagnetic Waves and Applications*, Vol. 24, No. 16, 2207–2221, 2010.

19. Pu, T., K.-M. Huang, B. Wang, and Y. Yang, "Application of micro-genetic algorithm to the design of matched high gain patch antenna with zero-refractive-index metamaterial lens," *Journal of Electromagnetic Waves and Applications*, Vol. 24, No. 8–9, 1207–1217, 2010.

20. Lim, S. and H. Ling, "Comparing electrically small folded conical and spherical helix antennas based on a genetic algorithm optimization," *Journal of Electromagnetic Waves and Applications*, Vol. 23, No. 11–12, 1585–1593, 2009.

21. Zhang, Y.-J., S.-X. Gong, and Y.-X. Xu, "Radiation pattern synthesis for arrays of conformal antennas mounted on an irregular curved surface using modified genetic algorithms," *Journal of Electromagnetic Waves and Applications*, Vol. 23, No. 10, 1255–1264, 2009.

22. Zhang, J., D. Huang, T. Lok, and M. Lyu, "A novel adaptive sequential niche technique for multimodal function optimization," *Neurocomputing*, Vol. 69, No. 16–18, 2396–2401, 2006.

23. Dilettoso, E. and N. Salerno, "A self-adaptive niching genetic algorithm for multimodal optimization of electromagnetic devices," *IEEE Transactions on Magnetics,* Vol. 42, No. 4, 1203–1206, 2006.

24. Lee, C., D. Cho, and H. Jung, "Niching genetic algorithm with restricted competition selection for multimodal function optimization," *IEEE Transactions on Magnetics*, Vol. 35, No. 3, 1722–1725, 1999.

25. Cho, D., J. Kim, H. Jung, and C. Lee, "Optimal design of permanent-magnet motor using autotuning niching genetic algorithm," *IEEE Transactions on Magnetics*, Vol. 39, No. 3, 1265–1268, 2003.

26. Tan, J., *Theory and Technology for Wire Rope Safe Detection*, 1st edition, Science Press, Beijing, China, 2009 (in Chinese).

27. Yang, S. and Y. Kang, *Theory and Technology for Wire Rope Broken Strands Quantitative Detection*, 1st edition, National Defense Industry Press, Beijing, China, 1995 (in Chinese).

28. American Society for Non-Destructive Testing, *Non-Destructive Testing Handbook*, 2nd edition, Electromagnetic, World Publishing Company, Shanghai, China, 1999 (in Chinese).